Computational Analysis of Tsunami Wave Run-Up by Implementation of TIMPULSE-SIM Model with Japan and Indonesian Seismic Tsunami

M.YASMIN REGINA[1], E. SYED MOHAMED[2]
[1]Civil Engineering,
B. S. Abdur Rahman Crescent Institute of Science and Technology,
Chennai, Tamil Nadu,
INDIA

[2]Computer Science and Engineering,
B. S. Abdur Rahman Crescent Institute of Science and Technology,
Chennai, Tamil Nadu,
INDIA

Abstract: - The alternative newly developed TIMPULSE-SIM model is used for forecasting all three phases of seismic/earthquake-induced tsunami waves. The main objective of this modeling is to predict the earliest arrival time of tsunami with less computation time. This paper analyses the third phase or the run-up phase of tsunami. The assessment of tsunami wave run-up minimize the risk in coastal community due to the tsunami impact. The paper introduces a closed set of algebraic expressions for modeling the run-up phase and the reliability of the model is analyzed by implementing and testing of this model to the two major historical seismic tsunami are, 2004 Indonesian Subduction zone tsunami in Indian ocean region, 2011 Great east Japan tsunami in Pacific ocean region. From this study, this proposed model should be a good alternative to the existing model for applying to the real time tsunami event because it includes the nonlinearity and frequency dispersion of wave, and applied to both near and far field tsunamis, efficient to apply for a long duration, mainly the computation time is achieved in O(minutes). More than 90 percentage of accuracy achieved in this model by validating the simulated results with the historical and other existing model that emphasize the model's reliability.

Key-Words: - TIMPULSE-SIM model, earthquake tsunami, impulsive disturbance, finite rectangular fault, earliest arrival time of tsunami, run-up,inundation distance, 2004 Indian Ocean tsunami, 2011 Tohoku tsunami.

Received: May 22, 2024. Revised: October 2, 2024. Accepted: November 4, 2024. Published: November 27, 2024.

1 Introduction

A tsunami is a powerful and often destructive natural phenomenon characterized by a series of ocean waves with extremely long wavelengths. These waves are typically triggered by underwater seismic activities such as earthquakes, volcanic eruptions, or underwater landslides, [1]. Tsunamis can travel across entire ocean basins and, upon reaching shallower coastal areas, can transform into massive and fast-moving waves. The run-up of a tsunami refers to the maximum height that the tsunami reaches above the normal sea level at a given location on the coastline depicted in Figure 1. It is a critical parameter in tsunami impact assessment and is measured from the shoreline to the highest point reached by the advancing waves.

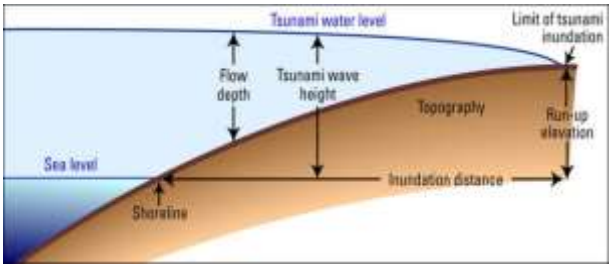

Fig. 1: Representation of tsunami run-up profile, [2]

Estimating tsunami run-up is crucial for effective disaster preparedness and risk reduction. Run-up, the maximum height reached by tsunami waves above normal sea level along the coast, guides infrastructure design, evacuation planning, and land-use regulations. Accurate predictions

inform the construction of resilient coastal structures, enable timely evacuation alerts, and shape community preparedness initiatives. The precise estimation of run-up is paramount for minimizing the impact of tsunamis, ensuring coastal safety, and fostering resilient coastal development practices.

Tsunamis pose a complex threat to coastal communities, with recent events prompting global concern and necessitating a reevaluation of tsunami hazard exposure. The devastating 2004 Indian Ocean Tsunami claimed over 2 lakh lives across 15 nations [3], and the more recent 2011 Tohoku Earthquake Tsunami resulted in an estimated 20,000 fatalities, [4], [5]. The aftermath of the 2004 tsunami spurred at-risk countries to reassess their preparedness measures, leading to an accelerated international focus on understanding the causes and impacts of tsunamis. Tsunamis emerge as secondary hazards resulting from various geophysical events. Tsunami inundation mapping relies on calculating potential run-up and inundation distances. Current run-up estimation methods often depend on empirical data, making their global application potentially unreliable. Thus, there is a need for a reliable, transparent, practical, and cost-effective method for accurately determining run-up and inundation distance.

This paper seeks to introduce a fundamental, conceptual tsunami run-up equation. It reviews existing run-up prediction methods and introduces a novel approach. The validity of the new run-up equation is verified with the historical tsunami data. In this study, the TIMPULSE-SIM model is applied to the two major historical tsunami events such as the 2004 Indian Ocean tsunami and the 2011 Tohoku, Japan tsunami for finding the run-up and inundation distances for the specified locations. The results obtained from this model are compared with historically observed data, and data from peer-reviewed literature for the historical tsunami events and to validate the efficacy of the proposed approach.

2 Existing Run-up Methods

Multiple techniques are employed to predict the run-up of a tsunami wave, denoting the peak vertical height it attains on the shore. A prevalent strategy involves leveraging numerical models, which simulate the tsunami wave's journey from its origin to coastal regions. These models meticulously consider various factors, including the initial sea surface displacement, bathymetry, and coastal topography. The models provide estimates of the expected tsunami wave run-up height upon reaching the beach using the above parameters. Physical model experiments to precisely determine the maximum wave run-up values in the early investigation of regular wave run-up. Pioneering research on wave run-up, formulating one of the earliest equations for its estimation provided. This formula posited that wave run-up is directly proportional to factors such as the Iribarren number, roughness factor, and porosity factor. A comprehensive study on natural beach dynamics, specifically exploring the relationships between swash, setup, and maximum wave run-up, [6], [7], [8]. It shows the total wave run-up as the sum of setup and half the swash height generated. The Iribarren number also recognized as the surf similarity parameter, holds significant importance in coastal engineering. It provides insights into the wave-breaking form, as the ratio of beach slope to wave steepness correlates with specific types of wave breaking—surging, collapsing, plunging, or spilling shown in Table 1. These classifications are contingent upon variations in wave steepness or slope angle. Researchers with varying perspectives on the complex wave run-up process have made major contributions to this field by introducing new formulas or updating previous work, [9], [10]. Deep-water waves change when they get closer to a shore with a slope gradient; they get shorter and steeper before breaking. The wave breaks, but its amplitude decreases as it moves up the beach. At the crest's highest point, the mean water surface experiences a minimum, identified as wave set-down. Subsequently, the water surface rises to the wave setup point, reaching the maximum wave setup elevation. The equation to determine both wave setup and set-down obtained from, [11].

Table 1. Iribarren number, [12]

Type of breaking	Iribarren number
surging wave	> 3.5
collapsing	3.0
plunging waves	0.5 to 3.0
spilling wave	< 0.5

Both analytical and numerical models for tsunami run-up, discussing the impact of tsunamis on beaches and the accuracy of the numerical model in simulating run-up is given in [13]. Overall, these papers collectively provide insights into the behavior and factors influencing the run-up of tsunamis, offering mathematical models and experimental data to understand and predict the run-up process.

Some of the existing numerical models that help in modeling of tsunami wave run-up phase are MOST model utilizes a linear shallow water equation without dispersion and is a widely used method for simulating real-time tsunami events, [14]. However, it is not accurately capture nonlinear effects. The computation time is O(hours). TSUNAMI N2 model is based on the linear long wave theory and solves the linear shallow water equations which are primarily used for near-field tsunami forecasting and warning systems. It has limited its applicability to far-field tsunami propagation and O(hours) of computation time, [15]. FUNWAVE model is a numerical model that solves the fully nonlinear Boussinesq equations and simulates wave propagation and transformation but may not be as efficient for large-scale or long-duration simulations, [16]. COMCOT model solves the nonlinear shallow water equations and assumes idealized conditions that may not capture all complexities of real-world events, such as variations in landslide characteristics or local bathymetry, [17]. The COULWAVE model is used to simulate the 28th November 2020 landslide tsunami, [18]. It combines a Coulomb-type model to simulate landslide motion with a tsunami propagation model. It may require specific input parameters related to the landslide characteristics and computation takes O(days).

3 Mathematical Formulation

One of the key factors in understanding the impact of tsunamis on coastal areas is the run-up of a tsunami wave. The run-up refers to the maximum vertical height that the tsunami wave reaches onshore. It is crucial to analyze the run-up of tsunami waves as it directly affects the extent of inundation and potential damage to coastal communities. In general, the prevailing approaches to determining the run-up of a tsunami wave integrate numerical modeling and empirical analysis, offering valuable insights into the potential repercussions of tsunamis on coastal regions. Figure 2 (Appendix) shows the framework of the TIMPULSE-SIM Model.

The innovative alternative model is developed for modeling the earthquake-generated tsunami wave behavior. This work is divided into three phases such as phase 1 - generation, phase 2 - propagation, and phase 3 - run-up. The model is named as TIMPULSE-SIM (Simulation Model for Tsunamis Induced by Impulsive Disturbances due to Earthquakes) and the main goal of this study is to develop a modeling of tsunami wave behavior through an analytical and geometrical approach using nonlinear theory on the surface of the ocean. The generation phase (Phase 1) modeling uses the impulsive force acting on the seabed to displace the enormous of seawater above this to generate a tsunami, [19]. The slip of the fault is considered gradually reduced along the rupture length and uniform along the fault width (variable slip model). The modeling of the initial displacement of seawater is done by using Euler's equation of motion because pressure and gravity force is only acting on the seawater. Phase 2, propagation of tsunami wave two two-dimensional models using Boussinesq approximation of solitary wave solution, here the wave is considered as a long, nonlinear, dispersive wave. The tsunami wave characteristics depend on the depth of the ocean. Initially the wave propagates as a cylindrical wave propagation in the orthogonal direction to the rupture movement. From the continuation of the above, phase 3 - the run-up phase of the tsunami wave is modeled with the help of the wave characteristics at the breaking point obtained from the propagation phase. Here, the new empirical equation is formulated for estimating the run-up height and inundation distance of tsunami waves towards the inland.

3.1 Assumptions

Consider the fluid domain is bounded in the vertical direction from $-h < z < \eta$ where h is the water depth of the ocean and η is a sea surface elevation. Water depth varies with space coordinates. It is unbounded in the horizontal directions $-\infty < x < \infty$, and $-\infty < y < \infty$. Assume the velocity of the water particles in the x and y direction $u_x = u_y$ and z direction is u_z. At time t=0, there is no disturbance, and the water particles in the ocean are considered in a rest or equilibrium condition. Therefore, $u_x = u_y = u_z = 0$ at t =0. It is assumed that the fluid is incompressible, inviscid, and irrotational. The seabed is considered as rigid and impermeable. The ocean has homogeneity in viscosity, gravity, and density. The pressure at the sea surface is zero and the pressure increases with the depth of the ocean. At the bottom of the seabed, there is no vertical velocity. The space is taken as Cartesian coordinates of 500 m spacing which then converted to spherical coordinates and the direction of wave propagation is measured with an angle

3.2 Generation and Propagation of Tsunami

TIMPULSE-SIM helps in modeling of three distinct phases of the tsunami (such as, generation, propagation, and run-up). The epicenter is taken as

the origin for modeling. Generation of tsunamis caused by the disturbance under the seabed which creates movement of the water particles. During the disturbance, the impulsive force acting on the water particle provides the velocity for particle movement by transferring energy from one to another neighboring water particles. A set of closed algebraic expressions helps in modeling of tsunami generation by dip-slip earthquake faults. Including all the other earthquake parameters (such as Magnitude, location, dip and slip angle, slip of fault), impulsive force generated by the seabed deformation also plays a major role in tsunami generation modeling. Here the linear Euler theory used for determining the sea surface deformation and their velocities with direction of movement (i.e. the initial tsunami wave) using the elastic dislocation of seabed deformation, [20], [21]. In the computation process, the generation area is subdivided into smaller areas using rupture velocity. The rupture velocity is chosen from 1 to 3 km/s, if the rupture velocity is 2km/s means the area is divided into 2km X 2km. The slip of fault is uniform along the width, and reducing towards the fault tip (along the length of rupture) i.e. variable slip along the fault line. The time for rupture is calculated from the focus the rupture propagation which will be used for finding the earliest arrival time of the tsunami.

TIMPULSE-SIM model uses the fully nonlinear Bousinessq equations with linear frequency dispersion [22] for the propagation phase of the tsunami and it is two-dimensional tsunami wave propagation. The propagation area is divided into small grids of 16.2" X 16.2" (i.e. 500m X 500m). The varying water depth in the area of propagation extracted from GEBCO, 2023 elevation data of 15 arc second interval grid. The wave propagated in a spherical coordinate system and the direction of wave propagation determined by the angle between the epicenter and the area where tsunami wave behavior needs to be predicted. The main goal of this study is to determine the earliest arrival time of a tsunami which is achieved by two approaches, (i) Propagation of tsunami wave in the specified direction (i.e. North, North-East, East, South-East, South, South-West, West, North-West), (ii) Propagation of tsunami wave in the shortest distance path (SDP) towards the specified area. This propagation phase ends when it satisfies any of the following conditions and it moves to the run-up phase,

(1) Wave reaches the coastline (the water depth of the ocean is greater than or equal to zero, $h \geq 0$)
(2) Wave breaks approaching the coastline (the point of wave breaking is the end of the propagation phase and initiation of the run-up phase)

At the end of the propagation phase, the following results are obtained, (i) Travel time of tsunami, (ii) Earliest arrival time of tsunami, (iii) maximum tsunami height, (iv) tsunami characteristics change along the wave propagation (wave length, wave celerity, and wave amplitude changes with water depth).

3.3 Tsunami Run-up phase

The run-up phase is modeled by a closed set of algebraic expressions using the results obtained from the propagation phase. The point of wave breaking or the point where the wave attained a maximum height is taken as an origin point for the run-up phase. The area of the run-up zone is divided into small grids, and the elevation data and topography data of each grid obtained from the GEBCO, 2023 elevation data of 15 arc second intervals. First, the slope of the beach (S_b) is estimated with the help of a linear curve fitting from the elevation of beach profile. The angle of the beach slope (θ_b) helps in mathematically deriving the beach profile. The beach slope profile is shown in Figure 3 and the height of changing water depth towards the coastline determined determined by,

$$h_x = dX * \tan\theta_b \quad (1)$$

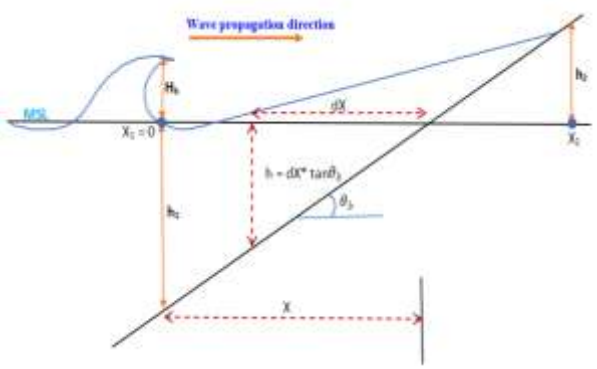

Fig. 3: Beach slope profile

The slope of the beach, S_b (or angle of beach slope, θ_b) is calculated using the bathymetry data GEBCO-2022 [23] 15" interval spacing in the modeling area for a specified location. The approaching tsunami wave height, water depth at the wave breaking point is obtained from the propagation phase. The approaching tsunami wave propagation is modeling in the horizontal x direction. The water depth and wave height is measured in vertical z-direction.

Figure 4 shows the representation of the run-up phase and the parameters utilized for formulating

the equation for estimating run-up height and inundation distance. H_b is the breaking wave height, d_b is the water depth at the point of wave breaking, W_{su} is the wave set-up, W_{sd} is the wave set down and θ_b is the angle of the beach slope. The slope of the beach, bathymetry profile of the beach, and topography data play an important role in this work.

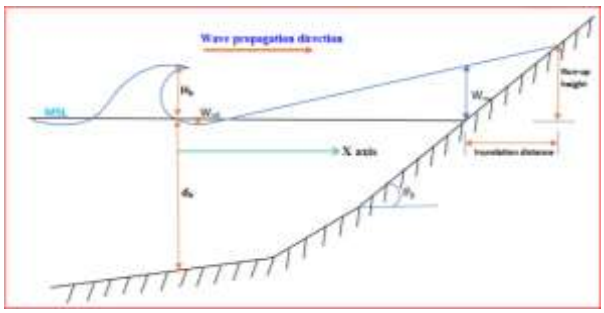

Fig. 4: Tsunami wave run-up phase diagram

In the context of water depth, the horizontal speed of water particles surpasses their vertical counterpart, leading to the adoption of (w = 0) to represent vertical velocity. At the free surface, the pressure (P) is designated as zero, and surface roughness is assumed to be negligible. The breaking of an approaching tsunami wave happens when the wave height is greater than or equal to 0.78 times the water depth. The wave set down at the breaking point and the wave set up at the coastline where water depth is zero is calculated. Using this information, the profile of the approaching water wave towards the land is determined using a linear curve fitting approach that helps to get the slope of the approaching wave estimated. This investigation focuses on simulating the run-up phase, employing the correlation between the beach slope and the slope formed by the approaching progressive wave line (S_w). The computation of S_w is achieved through the utilization of the following equation:

$$S_w = \frac{3}{8}\left(\frac{H_b}{d_b}\right)^2 \tan\theta_b \quad (2)$$

Where,
H_b = breaking wave height,
d_b = breaking water depth,
and A_b = angle of beach slope.

The empirical equation formulated (in the form of AX + BY + C = 0) for both the beach slope line and the approaching shoreline is solved to find the run-up and inundation of tsunami wave. The proposed empirical equation for finding the height of tsunami wave run-up (RU) in meters is given below:

$$RU = \frac{S_w.d_b - S_b.W_d}{S_w - S_b} \quad (3)$$

Where,
S_b is a slope of the beach (S_b = tan A_b),
and W_d = wave set down at the breaking point of wave (W_d = -(1/16)(H_b^2/d_b)). The proposed empirical equation for estimating Inundation distance by a tsunami wave is given below:

$$ID = \left[\frac{d_b - W_d}{S_w - S_b}\right] - \frac{d_b}{\tan\theta_b} \quad (4)$$

The outcomes obtained at the end of run-up phase modeling are, the beach profile of the local area, type of wave breaker, tsunami wave run-up height, and inundation distance, these help in predicting the area which is going to be affected by the tsunami. This will be useful for taking preventive measures to safeguard the environment and lives from the upcoming major destruction. The results obtained from this modeling are validated with the historical data collected from the US Geological Survey and the results from the literature. The tsunami wave characteristics are validated with the data collected from National Oceanic Atmospheric Administration tsunami database (NOAA), and the literature survey. The suitable results from this modeling show the applicability of this model for estimating tsunami run-up and inundation distance in both near shore and tele-tsunami.

The following are derived from this modeling study:

i. The height of tsunami generation does not only depend on the magnitude, slip of fault, dip angle but it depends on the water depth at the location.
ii. The initial tsunami height increases with increasing the slip of fault.
iii. Run-up increases increases with increasing the angle of the beach slope. The steep slope has more run-up height than the mild slope.
iv. Inundation distance decreases with increasing the angle of the beach. The distance that a tsunami propagates inward into the land is more for mild slopes than steep slopes.

Therefore, the inundation distance is more for Chennai than the Kanyakumari location for a 2004 Indian ocean tsunami. Because Chennai has mild slopes and Kanyakumari has steep slopes. However the wave height in Kanyakumari is higher than Chennai location due to these slope variations.

4 Case Studies

The reliability of this modeling approach is tested by implementing this model to the two significant seismic tsunami events. They are, the December 26, 2004, Indonesian subduction zone earthquake tsunami in the Indian Ocean, historically recorded as the most deadliest tsunami. Another one is March 11, 2011, the third major seismic tsunami in great east Japan. To validation of this modeling approach is done by comparing the simulated results with data from established sources such as the United States Geological Survey (USGS), National Oceanic Atmospheric Administration (NOAA), Tide gauge data, DART Buoy data, and peer-reviewed literature.

4.1 2004 Sumatra-Andaman Earthquake Tsunami

The 2004 Indian Ocean tsunami, one of the deadliest natural disasters in recorded history, was brought on by a massive undersea earthquake that struck off the coast of Sumatra on December 26. Reaching heights of more than 100 feet, the tsunami waves severely damaged coastal communities in 14 countries and claimed the lives of approximately 230,000 people. At 0:58:53 UTC, an earthquake with a magnitude of 9.3 occurred off the northern coast of Sumatra, Indonesia. This earthquake created a vertical rupture in the Burma tectonic plate's seabed, which caused the Burma plate to override the Indiana plate. This phenomenon spread to the Andaman Islands from northwest Sumatra. The earthquake's epicenter was located at 3.316 degrees North latitude and 95.854 degrees East longitude. The breach rapidly spread at a pace of 2.5 km/s, covering a tremendous radius of 1200 km in just 8 to 10 minutes which causing an uplift of 10 m and bottom subsidence of up to -6 m throughout 100–150 km broad across the subduction area, [24], [25], [26]. Over 15 countries that border the Indian Ocean were devastated on December 26, 2004, by what is possibly the worst tsunami in recorded history, [27].

Figure 5 provides a visual representation of the study area, facilitating a better understanding of the spatial dynamics associated with the 2004 Indian Ocean tsunami modeling efforts. A red mark denotes the epicenter of the tsunami, situated off the west coast of Sumatra, which serves as the focal point of the event's origin and a blue line delineates the rupture boundary of the 2004 Sumatra Andaman Earthquake, providing insight into the seismic activity that triggered the tsunami. The yellow marks indicate the specified locations selected for this study, indicating areas of interest for further investigation.

Fig. 5: Modeling study area of 2004, Indian Ocean tsunami. The red mark indicates the epicenter (off the west coast of Sumatra) and the blue line indicates the Rupture boundary line of the 2004 Sumatra Andaman Earthquake. The yellow mark indicates the specified location taken for this study

Table 2. The estimated values obtained from the generation phase of the 2004 tsunami

Sl. No.	Parameters	Values	References
1	Earthquake energy	3.35E+18 J	[28]
2	Seismic Moment	6.68E+22 Nm	[28]
3	Slip	8.612 m	[29]
4	Deep Ocean tsunami height	61.235 cm	[30]

Accurate estimation of parameters associated with the generation phase of the 2004 Indian Ocean tsunami is crucial for understanding the underlying mechanisms driving the event. Table 2 presents the estimated values of key parameters obtained from the TIMPULSE-SIM model for the generation phase of the 2004 tsunami. The earthquake energy is calculated to be approximately 3.35 × 10^18 joules, with a seismic moment of 6.68 × 10^22 newton-meters, as reported by the USGS in 2004. The below Figure 6 depicts the simulation of generation zone results obtained from the model. The slip, representing the relative displacement along the fault plane during the earthquake, is estimated to be 8.612 meters, the initial max tsunami height of 3m is estimated, and the deep ocean tsunami height is determined to be 61.235 centimeters, validation details shown in Table 2. The comparison between estimated values and reference values demonstrates a close agreement, indicating the accuracy of the estimations obtained from the TIMPULSE-SIM model.

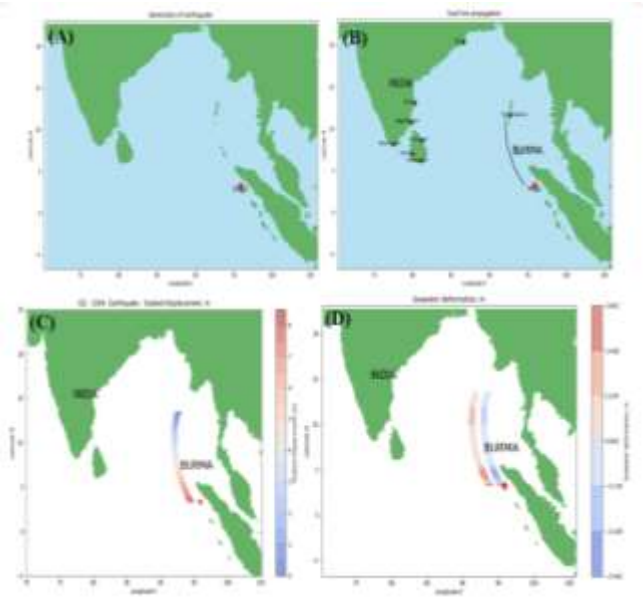

Fig. 6: Simulation results for the 2004 Indian Ocean tsunami

The tsunami reaches the coastline of India after 2 hours and 30 minutes of earthquake generation, Below Table 3 (Appendix) presents a tsunami travel time comparison between modeled data and historical observed data for various locations. The tsunami hit the coastline of Paradeep, Odisha in 2.47 hours after the tsunami generation i.e. 3:27:05 UTC or 8:57:05 IST, the tsunami hit the Cocos Island at 3:19:12 UTC, [29], [31] and the travel time was estimated as 2.3386 hours. The tsunami reached Chennai in 2.385 hrs at 3:22:01 UTC or 8:52:01 IST, [32]. Vishakhapatnam took 2.512 hours and reached at 3:29:39 UTC or 8:59:39 IST, [33]. Likewise in 0.6053 hours, the tsunami hit Portblair, Andaman Island at 1:35:12 UTC i.e. tsunami hit the coast after 36 minutes of the earthquake initiated, [34]. The accuracy of the model was over 90% when compared to the historical observed data. Overall, the comparison of actual and simulated tsunami travel periods shows how well the TIMPULSE-SIM model can replicate the dynamics of tsunami propagation in various kinds of geographic locations.

The tsunami travel time comparison between the simulated and historical observed data from Table 3 (Appendix) is shown graphically in Figure 7. The comparison shows that, for the most part, the simulated and historical tsunami travel times coincide closely, with a few minor exceptions.

Sumatra Andaman earthquake tsunami 2004 modeled results provided in Table 4 (Appendix). It depicts that Nagapattinam witnessed a substantial maximum wave height of 12.47 m, and an extensive inundation distance of 4400 m with a 4.38 m of run-up. and a maximum wave height of 7.41 meters estimated in Port Blair, Andaman. Chennai experienced a maximum wave height of 2.48 m, and a run-up height of 4.3 m with a 651 m inundation distance. These data contribute to a comprehensive understanding of tsunami wave dynamics and their effects on coastal regions.

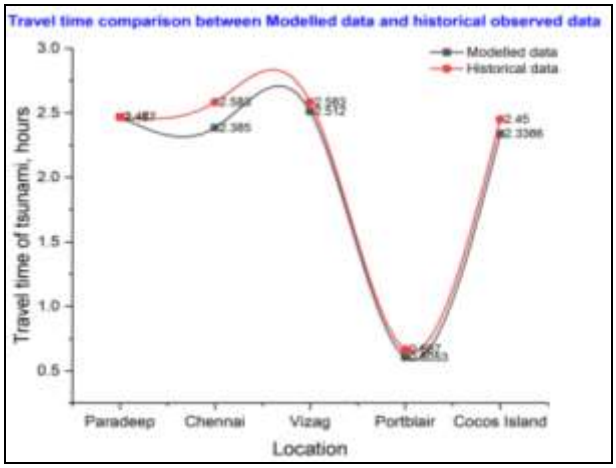

Fig. 7: Comparison graph of tsunami travel time between historical and modeled data from a 2004 tsunami in the Indian Ocean

In the 2004 Indian Ocean Tsunami, several parameters were compared between historical data, the TIMPULSE-SIM model, and existing models, with references to relevant literature. In Chennai, the tsunami height was historically between 2 to 3 meters. The TIMPULSE-SIM model estimated a height of 2.4762 meters, while the TSUNAMI-NSWE model predicted a height of 2.45 meters. For Nagapattinam, the historical run-up was recorded between 2 to 3.5 meters. The TIMPULSE-SIM model estimated the run-up at 4.38 meters, while the Boussinesq Model predicted it at 4.98 meters. For Cocos Island, the travel time historically recorded was 2.45 hours. The TIMPULSE-SIM model predicted a travel time of 2.3386 hours, while the FUNWAVE model predicted a travel time of 2.2667 hours and the TSUNAMI-N2 model estimated it at 2.4498 hours. The travel time to Nagapattinam was historically recorded at 2.5 hours, with the TIMPULSE-SIM model predicting 2.367 hours and the MIKE 21 model estimating 2.6167 hours [29], [37], [38].

Figure 8 represents the simulation results obtained from the TIMPULSE-SIM model when the tsunami wave propagate towards Chennai, Tamil Nadu India. The Figure 8(A) shows the visual representation of wave movement from the source to Chennai. The star mark indicates the epicenter of the earthquake. The blue line indicates a trace of tsunami wave propagation to Chennai which shows

the shortest distance from the generation zone to Chennai. Figure 8(B, C, D, E) shows the bathymetry changes and tsunami wave characteristics changes along the path of tsunami wave propagation. These indicate the changes depend on the depth of the ocean. Wave celerity decreases with decreasing water depth while wave height increases with decreasing the depth of the ocean. Therefore the wave height is very small in the deep ocean and it steeps at the coast causing more damage to the coastal community. The first wave to hit Chennai took 2.35 hours which is shown the Figure 8(C).

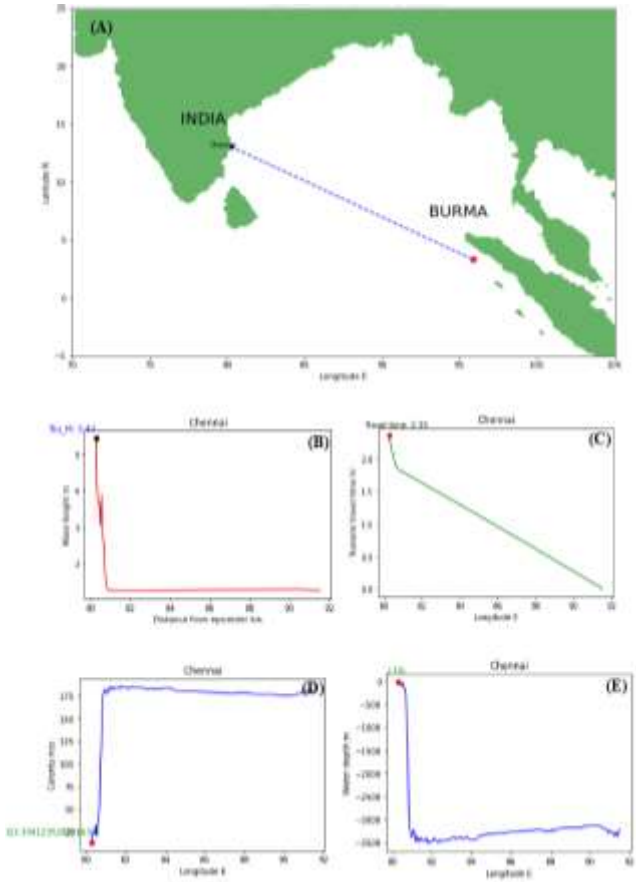

Fig. 8: Simulation results obtained from the TIMPULSE_SIM Model for the 2004 Indian Ocean tsunami

Figure 9 presents the estimated run-up and inundation distances at specified locations for the 2004 tsunami. The figure illustrates the spatial distribution of run-up heights and inundation distances across different coastal areas affected by the tsunami event. This visualization offers a clear depiction of the varying levels of tsunami impact along the coastline, highlighting areas with significant run-up heights and extensive inundation distances. Analyzing the spatial distribution of run-up and inundation distances can provide valuable insights into the tsunami's severity and its implications for coastal communities and infrastructure. From this study, the maximum run-up height of 5.16 m at Karaikal, Puthucherry and a maximum of 4400 m inundation distance at Nagapattinam is estimated that shown in Table 4 (Appendix).

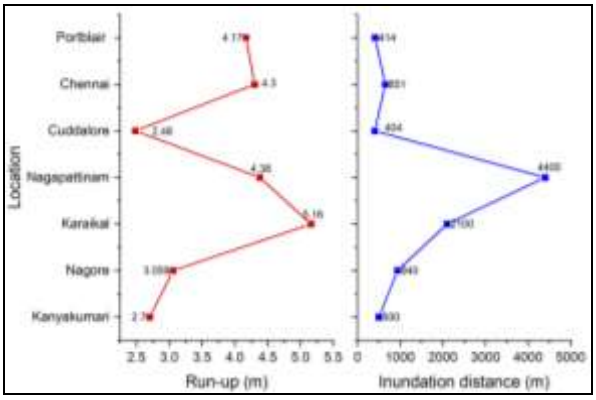

Fig. 9: Estimated Run-up and Inundation distance at the specified locations for the 2004 tsunami

Figure 10(a-e) in Appendix represents the simulated images obtained from this modelling for a tsunami wave spread in 30 mins (Figure 10a), 60 mins (Figure 10b), 90 mins (Figure 10c), 120 mins (Figure 10d), and 150 mins (Figure 10e) interval for a 2004 Indian Ocean tsunami.

4.2 2011 Tohoku, Japan Tsunami

In the Pacific Ocean, 72 kilometers east of the Shikawa Peninsula in the Tōhoku area of Japan, an earthquake with a magnitude of 9.0 to 9.1, [39] struck on March 11, 2011, at 14:46:23 Japan Standard Time (5:46:23 UTC). It caused a tsunami that lasted for around six minutes. It is referred to as the "Great East Japan Earthquake" occasionally. Miyagi Prefecture in northeastern Japan was the epicenter of the tsunami that occurred 130 km off the coast. The rupture area is estimated to be roughly 450 km × 200 km. According to the literature survey, this tsunami was the third major earthquake-generated tsunami this decade, [40], [41]; the other two were the Chilean tsunami [42] and the Sumatra tsunami, [43]. 20 minutes after the earthquake, the tsunami made landfall on the Japanese mainland, eventually damaging 2000 kilometers of the country's Pacific coast. Over 400 km2 of land were submerged by the tsunami. Particularly in the prefectures of Iwate, Miyagi, and Fukushima, the coastal communities were destroyed. The Geospatial Information Authority of Japan (GSI), [44], claimed that the tsunami's entire affected area along Japan's Pacific coast was 561

km2, while it is reported that the highest tsunami run-up height in Iwate Prefecture was 40 metres, [45]. The subduction zone plate boundary between the Pacific and North American plates is the source of the shallow thrust faulting that caused the M 9.1, Tohoku earthquake on March 11, 2011, which struck close to Honshu, Japan's northeast coast. The Pacific plate is moving around 83 mm/yr westward relative to the North American plate near the location of this earthquake. This movement started at the Japan Trench, which is located east of the earthquake on March 11, [46], [47]. The March 11th earthquake's location, depth (about 25 km), and focal mechanism solutions are all compatible with the event occurring on the subduction zone plate boundary. According to modeling of the earthquake's rupture, the fault shifted over a region that was around 400 km long (along strike) and 150 km wide in a down-dip direction, moving up to 50–60 m ,[48], [49].

Figure 11 illustrates the modeling study area for the 2011 Tohoku, Japan earthquake tsunami. A red mark signifies the epicenter of the earthquake, pinpointing the precise location where the seismic event originated. Additionally, a blue line is depicted to represent the plate boundary line associated with the 2011 Japan earthquake, indicating the tectonic boundary where significant seismic activity occurred.

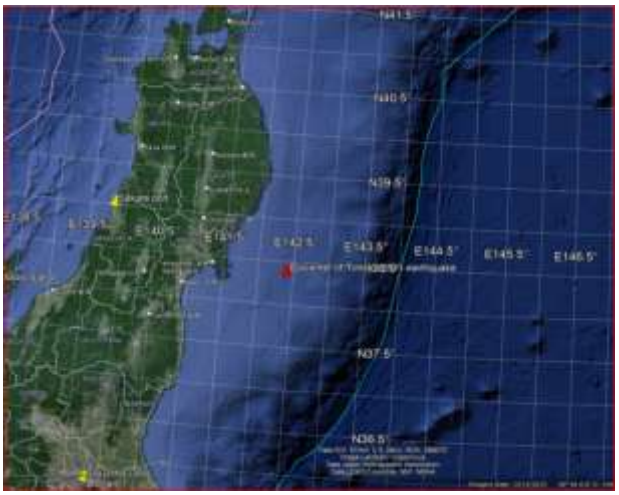

Fig. 11: Modeling study area for the 2011 Tohoku, Japan earthquake tsunami. The Red Mark indicates the epicenter, blue line indicates the plate boundary line of 2011 Japan earthquake

Table 5 presents the estimated results for the generation phase of the 2011 tsunami derived from the TIMPULSE-SIM model. The earthquake energy is estimated to be 2.82E+18 joules, with a seismic moment of 5.623E+22 newton-meters, based on data from the United States Geological Survey (USGS) in 2011. The deep ocean tsunami height is calculated to be 1.87 meters, and the slip, or the relative displacement along the fault line during the earthquake, is estimated to be 37.176 meters as shown in Figure 12, [40], [48], [50]. The precision of the estimations derived from the model is demonstrated by the good agreement between the estimated values and reference values.

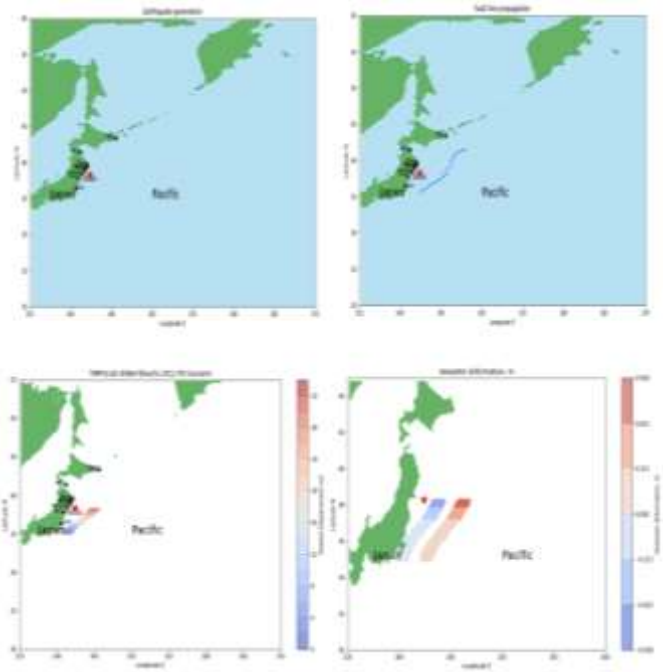

Fig. 12: Simulation results of modeling of generation zone for a 2011 Japan tsunami

Table 5. The results for the generation phase modeling of 2011 tsunami

Parameters	**Estimated Values**	**Reference**
Earthquake energy	2.82E+18 J	[48]
Seismic moment	5.623 X 10^{22} Nm	[48]
Max. Vertical slip, m	37.176 m	[50]

Table 6 (Appendix) presents a comparison of tsunami travel times between modeled data and historical data for various locations determined along the coastline of Japan. The tsunami hit the coastline of Tappi at 6:59:05 UTC, Hakodate at 7:21:12 UTC, Muroranko at 7:01:12 UTC, Chichijima Island at 7:22:32 UTC, and Yuki at 7:33:36 UTC validated with the data from National Oceanic Atmospheric Administration (NOAA, 2011). When compared with the historical observed data, the model achieved more than 95% accuracy.

Figure 13 provides the graphical representation of tsunami travel time comparison between the modeled data and the historical observed data for the 2011 Tohoku, Japan tsunami. The comparison reveals a close agreement between the modeled and historical tsunami travel times showing the applicability of the model in real-time tsunami events to forecast the tsunami wave characteristics. The results were validated by the NOAA, 2011.

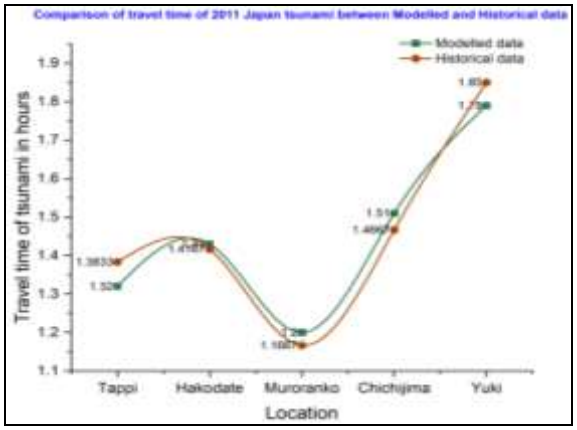

Fig. 13: Comparison of tsunami travel time (hours) between Modelled data and Historical data

Table 7 (Appendix) provides detailed information on the modeled tsunami wave characteristics at specified locations on the coastline of Japan for the 2011 Tohoku tsunami. Each location is identified by its latitude and longitude coordinates, facilitating precise geographical referencing. The travel time, run-up height, and inundation distance data are presented, aiding in the assessment of tsunami hazards and potential consequences for affected regions. From this study, a maximum wave height of 18.07 meters in Tokachi, Hokkaido, and 6.92 meters in Oarai, Ibaraki, greater than 10 meters in Iwate Prefecture, Miyagi Prefecture and Fukushima Prefecture have greater than 16 meters tsunami height estimated. In Ishinamoki, Miyagi, a maximum run-up height of 9 m, and 3.61 m in Tokachi, Hokkaido is estimated and the inundation distance is estimated between 200 to 560 for these locations, [45], [51], [52].

Figure 14 represents the simulation results obtained from the TIMPULSE-SIM model when the tsunami wave propagate towards Tokachi, Hokkaido, Japan. The Figure 14(A) shows the visual representation of wave movement from the source to Tokachi. The star mark indicates the epicenter of the earthquake. The blue line indicates a trace of tsunami wave propagation to Tokachi, Japan which shows the shortest distance from the generation zone to Tokachi. Figure 14(B, C, D, E) shows the bathymetry changes and tsunami wave characteristics changes along the path of tsunami wave propagation. These indicate the changes depend on the depth of the ocean. Wave celerity decreases with decreasing water depth while wave height increases with decreasing the depth of the ocean. Therefore the wave height is very small in the deep ocean and it steeps at the coast causing more damage to the coastal community. The first wave to hit the Tokachi took 1.21 hours which is shown the Figure 14 (C).

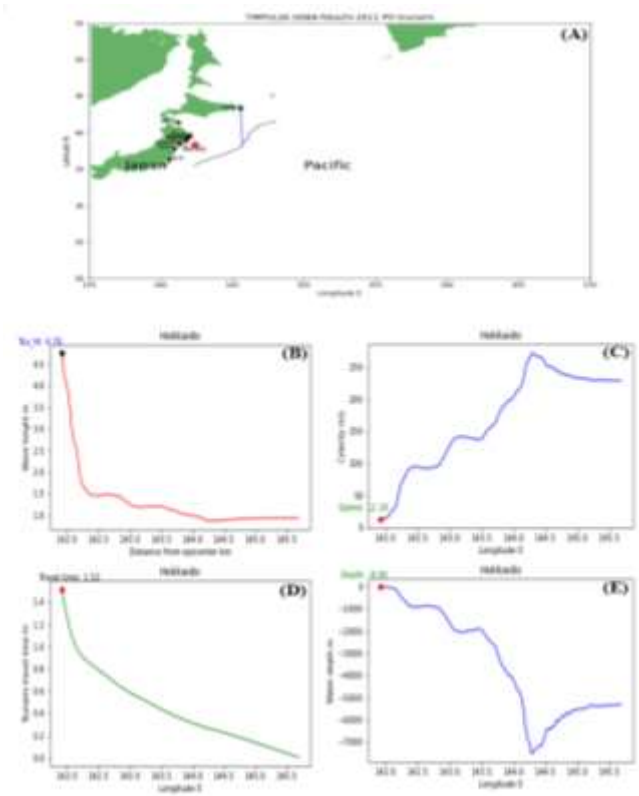

Fig. 14: Simulation results obtained from the model to reach Tokachi, Hokkaido Japan 2011

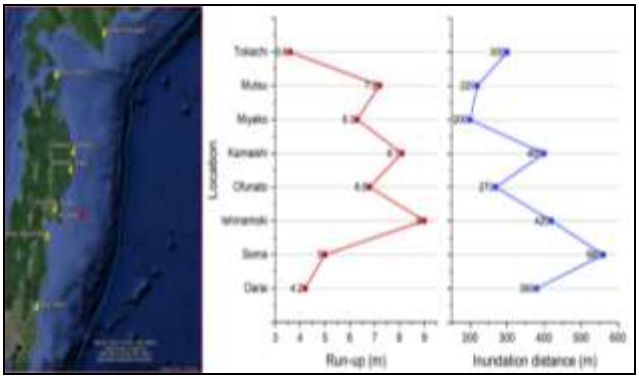

Fig. 15: Estimated tsunami Run-up and inundation distance in the coastline of Japan for 2011 tsunami

The predicted run-up and inundation distances for the 2011 Tohoku tsunami at the designated areas are shown in Figure 15. The image shows how the various coastal locations impacted by the massive tsunami event are distributed spatially in terms of run-up heights and inundation distances. This graphic provides a clear representation of the different tsunami impact levels throughout the coast, emphasizing locations with large run-up heights and long inundation distances. Understanding the spatial distribution of run-up and inundation distances can help determine how severe the tsunami will be and how it will affect infrastructure and coastal populations. From this study, the maximum run-up of 6 meters at Iwate Perfecture, 9 meters at Ishinamoki, Miyagi, and a maximum of 560 meters inundation distance at Soma, Fukushima are estimated and these are validated with [44], [49], [51], [52].

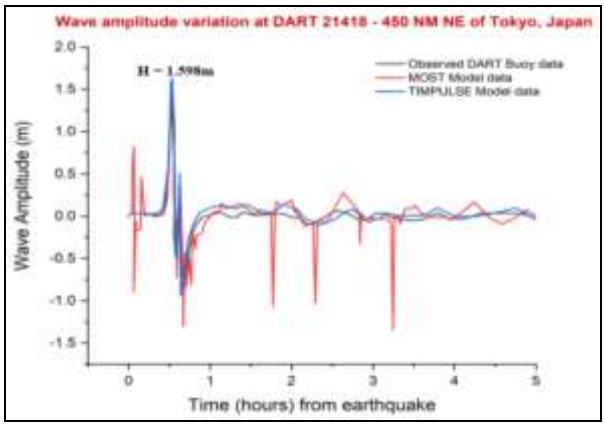

Fig. 16: Wave amplitude comparison at DART 21418, which is located 450 NM northeast of Tokyo, Japan

Figure 16 presents a comparative analysis of wave amplitudes at the location of DART 21418, situated approximately 450 nautical miles northeast of Tokyo, Japan. The figure juxtaposes wave amplitude data obtained from three different sources: DART BUOY data, MOST (Method of Splitting Tsunami) model data, and TIMPULSE-SIM model data. DART Buoy data observed the maximum wave height of 0.56 m at 0.524 hours (31 minutes 29 seconds) from the earthquake, MOST model data measures 1.564 m at 0.5375 hours (32 minutes 15 seconds), and the TIMPULSE-SIM model data estimated a maximum wave height of 1.58 m at 0.52024 hours 31 minutes 13 seconds. Through comparative analysis and validation against observed data, the TIMPULSE-SIM model has exhibited commendable performance in accurately simulating wave characteristics, including amplitude, travel time, and inundation distance, as evidenced by its close agreement with DART Buoy measurements and other modeling methodologies such as the MOST model.

Figure 17(a-e) in Appendix represents the simulated images of tsunami wave spread obtained from this modelling for a 2011 Tohoku, Japan tsunami in the time interval of 30 mins (Figure 17a), 60 mins (Figure 17b), 90 mins (Figure 17c), 120 mins (Figure 17d), and150 mins (Figure 17e).

5 Comparative Analysis of Results

The following are derived by analyzing the results of two tsunami events such as the Sumatra-Andaman earthquake tsunami of 2004 and the Tohoku, Japan tsunami of 2011.

5.1 Generation Phase

The below table shows the modeled results obtained from the two tsunami events in the generation phase of the tsunami. The parameters mentioned in Table 8 are responsible for the tsunami generation. Both events have similar magnitude of the earthquake, but the changes in fault parameters cause the variations in a slip of fault and subsequent tsunami initiation. Slip is directly proportional to the magnitude. But other parameters, such as fault area affects the slip i.e increasing fault area reduces the fault slip. Table 8 depicts the generation phase results of two tsunami events. It provides the area of fault is more for the 2004 Sumatra tsunami than the 2011 Japan tsunami, therefore slip is more for the 2011 Japan tsunami. The angle of dip directly proportional to slip of fault. In 2011 Japan tsunami had a higher magnitude of 9.1, but fault area and angle of dip were small compared to the 2004 tsunami.

Table 8. Comparison of generation phase results for 2004 and 2011 tsunami events

Parameters	2004, Sumatra tsunami	2011, Japan Tsunami
Magnitude	9.15	9.1
Fault length, km	1200	500
Fault width, km	90	108
Focal depth, km	30	29
Dip angle, degree	8	15
Slip of fault, m	8.61	33.45
Water depth in origin, m	3362	5837
Initial tsunami height, m	3.6	0.938

Therefore the fault slip was more in the 2011, Tohoku, Japan tsunami. The parameters which

influence the height of tsunamis are fault slip and depth of the ocean at the location.

Fault slip is more in the 2011 tsunami but the water depth at the location is measured as 5800 m. Hydrostatic pressure at the location influences the height of tsunami initiation. In the 2004 tsunami scenario, the slip was less and the water depth was low compared to the 2011 tsunami caused the maximum height of tsunami initiation.

5.2 Propagation Phase

Once the tsunami is initiated, it propagates outward from the generation zone and the direction of propagation is orthogonal to the rupture direction. The characteristics of tsunami waves depend on the water depth variations in the ocean, [53]. The tsunami wave height increases with decreasing water depth. Table 9 shows the propagation phase results for the two tsunami events. In 2004 scenario, the bathymetry variation toward Chennai gradually reduces from 3000 m but in the 2011 scenario, it changes from approximately 6000 m towards Hokkaido. Therefore the deep ocean wave height was lower in the Japan tsunami compared to the 2004 Indian Ocean tsunami. Tsunami wave celerity is more in the deep ocean, it diminishes in reducing water depth. 2011 tsunami event had higher wave celerity than the other event due to this bathymetry variation.

Table 9. Comparison of generation phase results for 2004 and 2011 tsunami events

Parameters	2004, Indian tsunami	2011, Japan Tsunami
Location	Chennai	Hokkaido
Wave height, m	1.6	0.93
Wavelength,km	391.6584	1382.8211
Wave period	00:36:17	01:35:51
Celerity, km/hr	647	865

5.3 Run-up Phase

The below Figure 18 shows the slope variations along the Chennai and Kanyakumari beach lines in Tamil Nadu, India. In Chennai, the slope is gradually reducing from deep to shallow ocean, but in Kanyakumari, the water depth is suddenly increasing causing the steep slope which makes the sudden increase in tsunami height, and then the slope gently varies.

The run-up phase results obtained from the 2004 Indian Ocean tsunami for three different beach slope conditions are given in Table 10. The three locations were taken for comparison, Chennai has a gradually varying slope, Nagapattinam has a plain terrain the angle of the beach slope is less than a degree, and Kanyakumari has a gentle slope condition. If the beach slope is small, the inundation distance is high. The beach slope in Chennai is more compared to Nagapattinam. Therefore, Nagapattinam has a higher inundation distance than Chennai and Kanyakumari. The tsunami height is higher on steep slopes but the inundation distance is less, therefore Kanyakumari has less inundation distance than other locations.

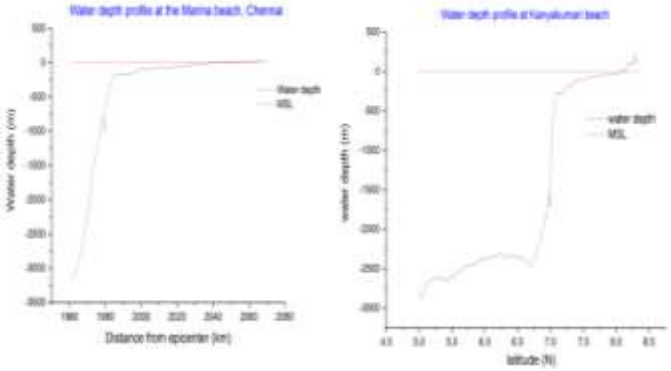

Fig. 18: The slope variations in Chennai and Kanyakumari on the coastline of Tamil Nadu, India

Table 10. The run-up phase variation for a different beach slope condition for a 2004 tsunami

Parameters	Beach slope	Run-up, m	Inundation distance, m
Nagapattinam	plain terrain	4.38	4400
Chennai	Gradual slope	4.3	651
Kanyakumari	Gentle slope	2.7	500

6 Conclusion

This paper presents TIMPULSE-SIM, an alternative computational model designed to simulate earthquake-induced tsunamis with a particular focus on the crucial run-up phase. The model employs a three-phase approach, encompassing generation, propagation, and run-up, to accurately predict tsunami wave behavior. The following are the main advantages of using the TIMPULSE-SIM Model are, (i) TIMPULSE-SIM model uses the linear frequency dispersion, therefore the tsunami wave (or solitary wave) characteristics change with depth is estimated effectively, (ii) It includes the nonlinearity of the equation which plays a crucial role in modeling of shallow water wave propagation (like tsunamis) and their coastal impact (i.e. it accounts the wave breaking effects), (iii) It can be applicable for both distant and local tsunamis. It helps in simulating

near-field tsunami as well as far field tsunami, (iv) It simulate the long duration or large scale tsunami. The computation time for tsunami simulation is O(minutes). (v) Mainly It requires the minimum input parameters for forecasting the tsunami wave behavior. The tsunami can be simulated using the preliminary available earthquake parameters (such as, Magnitude, origin location, origin time, and focal depth).

In this paper, the TIMPULSE-SIM model is applied to the two major tsunami events, and the tsunami wave behaviour were analyzed in depth. One is 2004 Sumatra-Andaman earthquake tsunami and the another one is 2011 Tohoku, Japan tsunami both are historical recorded most destructive tsunamis. The parameters which are highly influences the tsunami wave behaviour analyzed. The generation of tsunami depends on the magnitude, fault area, fault slip and water depth at the location. The propagation phase of tsunami depends on the bathymetry variation of ocean. The run-up of tsunami depends on the slope variation along beach line. The results are validated with the observed data, and existing tsunami model proves their reliability of applying in real time tsunami events and computation time for estimation measured as O(minutes) helps in tsunami forecasting and disaster preparedness.

Declaration of Generative AI and AI-assisted Technologies in the Writing Process

During the preparation of this work the authors used Grammarly for language editing. After using this service, the authors reviewed and edited the content as needed and take full responsibility for the content of the publication.

References:

[1] Regina M. Y., and Mohamed E. S., Modeling study of tsunami wave propagation, *International Journal of Environmental Science and Technology, 20, 1,* 10491 - 10506,2022, https://doi.org/10.1007/s13762-022-04484-2.

[2] Tsunami terms, Pacific Coastal and Marine Center, USGS, 2010, [Online]. https://www.usgs.gov/media/images/tsunami-terms (Accessed Date: November 5, 2024).

[3] Regina MY, Mohamed ES, Modeling and analysis of tsunami wave propagation characteristics in the coast of Bay of Bengal. *Adv Intell Syst Comput,* 1408. Springer, Singapore, 2022. https://doi.org/10.1007/978-981-16-5157-1_50.

[4] Nobuhito Mori, Tomoyuki Takahashi and the 2011 Tohoku earthquake tsunami Joint Survey Group, Nationwide Post Event Survey and Analysis of the 2011 Tohoku Earthquake Tsunami, *Coastal Engineering Journal*, 54:1, 1250001-1-1250001-27, 2012, https://doi.org/10.1142/S0578563412500015.

[5] Guha-Sapir D, Hoyois Ph., Below. R. Annual Disaster Statistical Review 2015: The Numbers and Trends. *Brussels: CRED*; 2016. http://dx.doi.org/10.13140/RG.2.2.10378.88001.

[6] Granthem, K. N., Wave Run-up on sloping structures. Eos, *Transactions American Geophysical Union*, 34(5), 720-724, 1953. https://doi.org/10.1029/TR034i005p00720.

[7] Hunt, I.A., Design of seawalls and breakwaters, *J. Waterway Harbors Coastal Eng. ASCE*, 85, 123-152, 1959. https://doi.org/10.1061/JWHEAU.0000129.

[8] Holman, R.A. and A.H. Sallenger., Setup and swash on a natural beach, *Journal of Geophysical Research*, 90(C1), 945-953, 1985. https://doi.org/10.1029/JC090iC01p00945.

[9] Battjes, J. A., Surf similarity, *Proc. 14th Conf. Coastal Engineering (Copenhagen)*, New York, ASCE, Copenhagen, Denmark, June 24-28, 1974, pp. 466–480. https://doi.org/10.1061/9780872621138.029.

[10] Peter Nielsen, & David J. Hanslow, Wave Runup Distributions on Natural Beaches, *Journal of Coastal Research*, Vol. 7, issue 4, Pages: 1139-1152, 1991, [Online]. http://www.jstor.org/stable/4297933. (Accessed Date: November 5, 2024).

[11] Smith, J. M. and Vincent, C. L., Equilibrium ranges in surf zone wave spectra, *J. Geophys. Res*., 108, C11, 3366, 2003. DOI: 1029/2003 JC001930.

[12] Tom Bruce, Jentsje Van Der Meer, Tim Pullen, and William Allsop, Chapter 23: Wave Overtopping at Vertical and Steep Structures, *Handbook of Coastal and Ocean Engineering*, pp. 633-661, 2018. https://doi.org/10.1142/9789813204027_0023.

[13] Madsen, P. A., Fuhrman, D. R., and Schaffer, H. A., On the solitary wave paradigm for tsunamis. *Journal of Geophysical Research: Oceans*, *113* (C12), 2008. https://doi.org/10.1029/2008JC004932.

[14] Vasily Titov, Utku Kânoglu, Ph.D.2; and Costas Synolakis, Development of MOST for Real-Time Tsunami Forecasting. *J. Waterway, Port, Coastal, Ocean Eng.*, 2016, 142(6): 03116004, 2016. https://doi.org/10.1061/(ASCE)WW.1943-5460.0000357.

[15] Shailesh Nayak and T. Srinivasa Kumar, Indian Tsunami Warning System. *The International Archives of the Photogrammetry, Remote Sensing and Spatial Information Sciences,* Vol. XXXVII, Part B4, pp: 1501-1506, Beijing 2008. ISSN 1682-1750.

[16] I. E. Mulia, S. Watada, T. C. Ho, K. Satake, Y. Wang, & A. Aditiya,. Simulation of the 2018 tsunami due to the flank failure of Anak Krakatau volcano and implication for future observing systems. *Geophysical Research Letters*, 47, e2020GL087334, 2020. https://doi.org/10.1029/2020GL087334.

[17] Jun-Whan Lee, Eun Hee Park, Sun-Cheon Park and Seung-Buhm Woo, Development of the Global Tsunami Prediction System using the Finite Fault Model and the Cyclic Boundary Condition. *Journal of Korean Society of Coastal and Ocean Engineers,* 27(6), pp. 391-405, Dec. 2015. http://dx.doi.org/10.9765/KSCOE.2015.27.6.391.

[18] M. Geertsema, B. Menounos, G. Bullard, J. L. Carrivick, J. J. Clague, C. Dai, D. Donati, G. Ekstrom, J. M. Jackson, P. Lynett, M. Pichierri, A. Pon, D. H. Shugar, D. Stead, J. Del Bel Belluz, P. Friele, I. Giesbrecht, D. Heathfield, T. Millard, S. Nasonova, A. J. Schaeffer, B. C. Ward, D. Blaney, E. Blaney, C. Brillon, C. Bunn, W. Floyd, B. Higman, K. E. Hughes, W. McInnes, K. Mukherjee, and M. A. Sharp, The 28 November 2020 landslide, tsunami, and outburst flood – A hazard cascade associated with rapid deglaciation at Elliot Creek, British Columbia, Canada. *Geophysical Research Letters*, 49(6), e2021GL096716, 2022. https://doi.org/10.1029/2021GL096716.

[19] E. S. Mohamed and M. Y. Regina, Computation Model to forecast the tsunami wave propagation by 2-dimensional Multi-Resolution Cellular Automata for the 2004 Indian Ocean tsunami, *2022 3rd International Conference on Computation, Automation and Knowledge Management (ICCAKM)*, Dubai, United Arab Emirates, 2022, pp. 1-7, https://doi.org/10.1109/ICCAKM54721.2022.9990439.

[20] Okada, Y., Surface deformation due to shear and tensile faults in a half-space, *Bull. seism. Soc. Am.,* 75 (4), 1135–1154, 1985. https://doi.org/10.1785/BSSA0750041135.

[21] Mansinha, L. and Smylie, D.E., The displacement field of inclined faults, *B. seism. Soc. Am.*, 61 (5), 1433–1440, 1971. https://doi.org/10.1785/BSSA0610051433.

[22] B. Poisson, C. Oliveros, and R. Pedreros, Is there a best source model of the Sumatra 2004 earthquake for simulating the consecutive tsunami?, *Geophys. J. Int*., 2011, 185, issue 3, 1365–1378. https://doi.org/10.1111/j.1365-246X.2011.05009.x.

[23] GEBCO Compilation Group,*GEBCO_2022*, 2022 Grid, https://doi.org/10.5285/e0f0bb80-ab44-2739-e053-6c86abc0289c.

[24] Eric L. Geist, Vasily V. Titov, and Costas E. Synolakis, Tsunami: wave of change, *Scientific American,* Vol. 294, issue 1, pages 56-63, February 2006.. https://doi.org/10.1038/scientificamerican0106-56.

[25] Ioualalen, M., Asavanant, J., Kaewbanjak, N., Grilli, S. T., Kirby, J. T., & Watts, P., Modeling the 26 December 2004 Indian Ocean tsunami: Case study of impact in Thailand. *Journal of Geophysical Research: Oceans*, 112(C7), 2007. https://doi.org/10.1029/2006JC003850.

[26] C. J. Ammon , C. Ji, H. Thio, D. Robinson, S. Ni, V. Hjorleifsdottir, H. Kanamori, T. Lay, S. Das, D. Helmberger, G. Ichinose, J. Polet, and D. Wald, Rupture process of the 2004 Sumatra-Andaman earthquake, *Science*, 308(5725):1133-9, 2005. https://doi.org/10.1126/science.1112260.

[27] A. Suppasri, N. Shuto, F. Imamura, S. Koshimura, E. Mas and A. C. Yalciner, Lessons Learned from the 2011 Great East Japan Tsunami: Performance of Tsunami Countermeasures, Coastal Buildings, and Tsunami Evacuation in Japan. *Pure Appl. Geophys,* 170, 993–1018, 2013. https://doi.org/10.1007/s00024-012-0511-7.

[28] USGS, *Pacific Coastal and Marine Center*, Tsunami Generation from the 2004, M=9.1 Sumatra-Andaman Earthquake, [Online]. https://www.usgs.gov/centers/pcmsc/science/tsunami-generation-2004-m91-sumatra-andaman-earthquake (Accessed Date: November 5, 2024).

[29] Stephan T. Grilli, Mansour Ioualalen, Jack Asavanant, Fengyan Shi, James T. Kirby, and Philip Watts, Source Constraints and Model Simulation of the December 26, 2004, Indian Ocean Tsunami,*Journal of Waterway, Port, Coastal, Ocean Engineering*, 133(6): 414-428, 2007. https://doi.org/10.1061/(ASCE)0733-950X(2007)133:6(414).

[30] Diego Arcas and Vasily Titov, Sumatra tsunami: lessons from modeling. *Surv Geophys*, 27:679–705, 2006. https://doi.org/10.1007/s10712-006-9012-5.

[31] National Geophysical Data Center / World Data Service: NCEI/WDS Global Historical Tsunami Database. *NOAA National Centers for Environmental Information, 2023.* http://dx.doi.org/10.7289/V5PN93H7.

[32] Narayan J P, Sharma M L, Maheshwari B K, Run-up and inundation pattern developed during the Indian Ocean tsunami of December 26, 2004 along the coast of Tamilnadu (India), *Gondwana Res Gondwana Newsl,* Sect, 8(4), 611–616, 2005. https://doi.org/10.1016/S1342-937X(05)71162-X.

[33] Alpa Sheth, Snigdha Sanyal, Arvind Jaiswal, and Prathibha Gandhi, Effects of the December 2004 Indian Ocean Tsunami on the Indian Mainland. *Earthquake Spectra*, Vol. 22, No. S3, pages S435–S473, 2006. https://doi.org/10.1193/1.2208562.

[34] Yong-Sik Cholakshumanan, Chokkalingam Lakshumanan, Chokkalingam Byung Ho Choi, A Field Report on the Impact of the 2004 Sumatra Tsunami Along the Southeast Coast of India, *Coastal Engineering in Japan*, March 2009, 51(01). https://doi.org/10.1142/S057856340900193X.

[35] R. Rajaraman, S. Joseph Winston, T. S. Murty, Hema Achyuthan, and N. Nirupama, Numerical Simulation of Tsunamis on the TamilNadu Coast of India,Marine Geodesy, 29: 167–178, 2006, https://doi.org/10.1080/01490410600939199.

[36] Sundar V, Sannasiraj S A, Murali K, Sundaravadivelu R., Run-up and inundation along the Indian Peninsula, including the Andaman Islands, due to the Great Indian Ocean Tsunami. *J Waterw Port Coast Ocean Eng,* 133:401–413, 2007. https://doi.org/10.1061/(ASCE)0733-950X(2007)133:6(401).

[37] M. H. Dao and P. Tkalich, Tsunami propagation modeling – a sensitivity study, Natural Hazards and Earth System Sciences, Vol. 7, issue 6, pages: 741–754, 2007. https://doi.org/10.5194/nhess-7-741-2007.

[38] G. Gopinath, F. Lovholt, G. Kaiser, C. B. Harbitz, K. Srinivasa Raju, M. Ramalingam, and Bhoop Singh, Impact of the 2004 Indian Ocean tsunami along the Tamil Nadu coastline: field survey review and numerical simulations. *Natural Hazards*, 72, 743–769, 2014. https://doi.org/10.1007/s11069-014-1034-6.

[39] Koshimura Shunichi and Shuto Nobuo, Response to the 2011 Great East Japan Earthquake and Tsunami disaster, *Phil. Trans. R. Soc. A.,* 373, 20140373, 2015, http://doi.org/10.1098/rsta.2014.0373.

[40] Mori, N., Takahashi, T., Yasuda, T., and Yanagisawa, H., Survey of 2011 Tohoku earthquake tsunami inundation and run-up. *Geophysical Research Letters,* vol. 38, L00G14, pp.1-6, 2011. https://doi.org/10.1029/2011GL049210.

[41] Mori, N., Cox, D. T., Yasuda, T., and Mase, H., Overview of the 2011 Tohoku Earthquake Tsunami Damage and Its Relation to Coastal Protection along the Sanriku Coast. *Earthquake Spectra*, 29(S1), S127-S143, 2013. https://doi.org/10.1193/1.4000118

[42] L. Faenza, and A. Michelini, Regression analysis of MCS intensity and ground motion parameters in Italy and its application in Shake Map, *Geophys. J. Int.*, 180 (3), pp. 11381152, 2010. https://doi.org/10.1111/j.1365-246X.2009.04467.x.

[43] Okayasu, A., Shimozono, T., Sato, S., Tajima, Y., Liu, H., Takagawa, T., & Fritz, H. M., 2011 Tohoku Tsunami Runup And Devastating Damages Around Yamada Bay, Iwate: *Surveys And Numerical Simulation. Coastal Engineering Proceedings,* 1(33), currents.4, pp.1-14, 2012. https://doi.org/10.9753/icce.v33.currents.4.

[44] Geospatial Information Authority of Japan (GSI), 2011a, [Online]. (http://www.gsi.go. jp/) (Accessed Date: November 5, 2024).

[45] Shunichi Koshimura, Satomi Hayashi, and Hideomi Gokon, The impact of the 2011 Tohoku earthquake tsunami disaster and implications to the reconstruction, *Soils and Foundations,* 54(4), 560–572, 2014. http://dx.doi.org/10.1016/j.sandf.2014.06.002.

[46] K. Goto, K. Fujima, D. Sugawara. S. Fujino, K. Imai, R. Tsudaka, T. Abe and T. Haraguchi, Field measurements and numerical modeling for the run-up heights and inundation

distances of the 2011 Tohoku-oki tsunami at Sendai Plain, Japan, *Earth Planet,* Sp 64, 1247–1257, 2012. https://doi.org/10.5047/eps.2012.02.007.

[47] Sato S., Characteristics of the 2011 Tohoku Tsunami and introduction of two level tsunamis for tsunami disaster mitigation. *Proc Jpn Acad Ser B Phys Biol Sci*. 91(6), 262-72, 2015. PMID: 26062739; PMCID: PMC4565975. https://doi.org/10.2183/pjab.91.262

[48] USGS, M 9.1 - 2011 Great Tohoku Earthquake, Japan. *Earthquake Hazards Program*, 2023, [Online]. https://earthquake.usgs.gov/earthquakes/eventpage/official20110311054624120_30/executive. (Accessed Date: November 5, 2024).

[49] Lay T, Kanamori H. 2011 Insights from the 2011 great Japan earthquake. *Phys. Today,* 64, 33–39, 2011. https://doi.org/10.1063/PT.3.1361.

[50] Fujii, Y., Satake, K., Sakai, S., Shinohara, M., and Kanazawa, T., Tsunami source of the 2011 off the Pacific coast of Tohoku Earthquake. *Earth, Planets and Space,* 63(7), 815-820, 2011. https://doi.org/10.5047/eps.2011.06.010.

[51] Lekkas, E. Andreadakis, I. Kostaki and E. Kapourani, Critical Factors for Run-up and Impact of the Tohoku Earthquake Tsunami, *International Journal of Geosciences*, Vol. 2 No. 3, pp. 310-317, 2011. http://dx.doi.org/10.4236/ijg.2011.23033.

[52] M. Chini, A. Piscini, F. R. Cinti, S. Amici, R. Nappi and P. M. DeMartini, The 2011 Tohoku (Japan) Tsunami Inundation and Liquefaction Investigated Through Optical, Thermal, and SAR Data, in *IEEE Geoscience and Remote Sensing Letters*, vol. 10, no. 2, pp. 347-351, March 2013, https://doi.org/10.1109/LGRS.2012.2205661.

[53] Yasmin Regina M and Syed Mohamed E, Study on Analytical Modeling of Tsunami Wave Propagation, *Advances in Parallel Computing*, Vol. 37, 479-494, 2020. https://doi.org/10.3233/APC200188.

Contribution of Individual Authors to the Creation of a Scientific Article (Ghostwriting Policy)

- E. Syed Mohamed conceptualized, provided guidance, oversight, and supervision throughout the study. Reviewed, and approved the manuscript.
- Yasmin Regina M. Collected data, and performed analysis under the guidance of the supervisor, Dr. E. Syed Mohamed. Contributed substantially to the drafting and writing of the manuscript. Reviewed and revised the manuscript based on feedback.

Sources of Funding for Research Presented in a Scientific Article or Scientific Article Itself

No funding was received for conducting this study.

Conflict of Interest

The authors have no conflicts of interest to declare.

APPENDIX

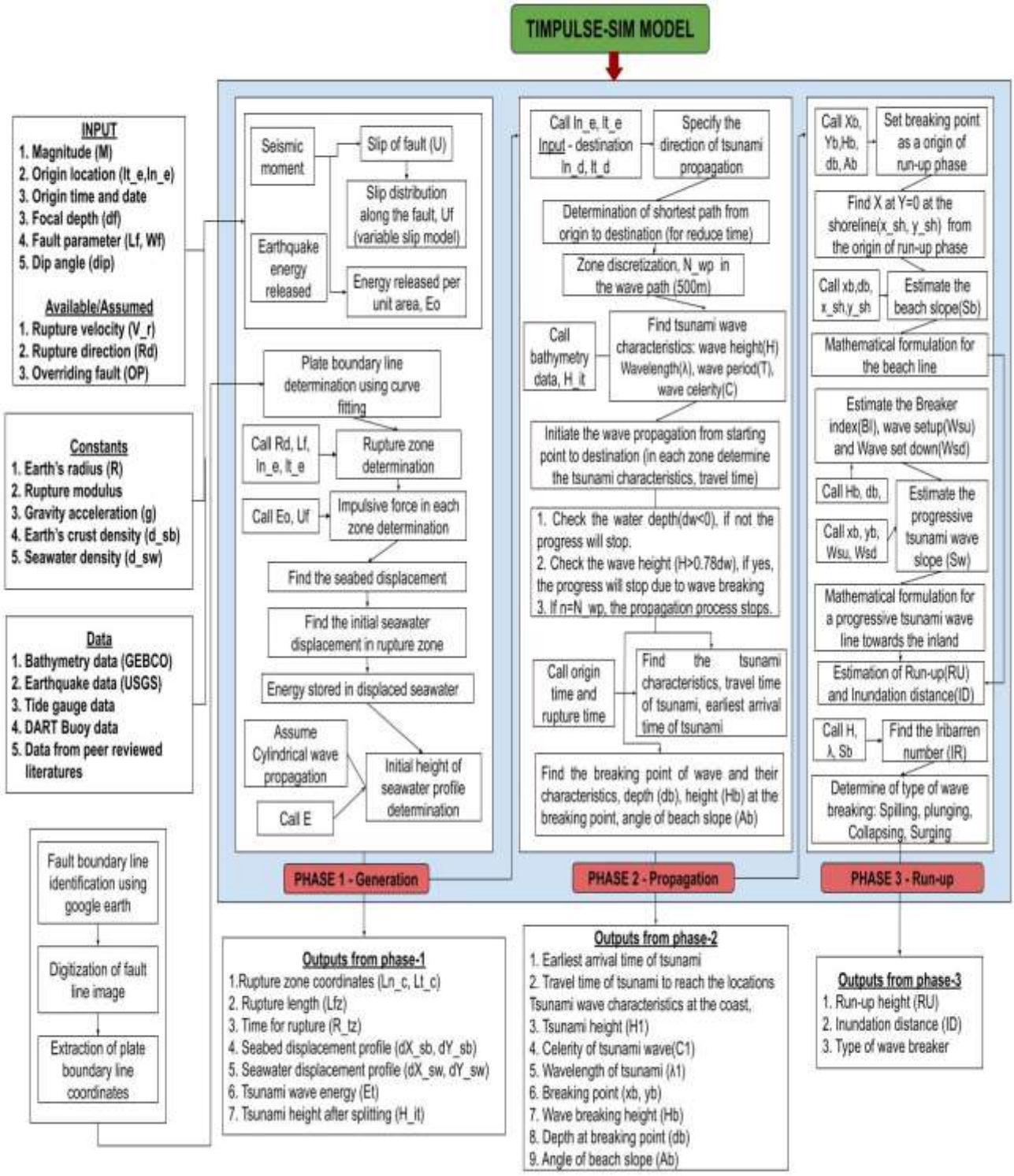

Fig. 2: Proposed Framework for TIMPULSE-SIM Model development

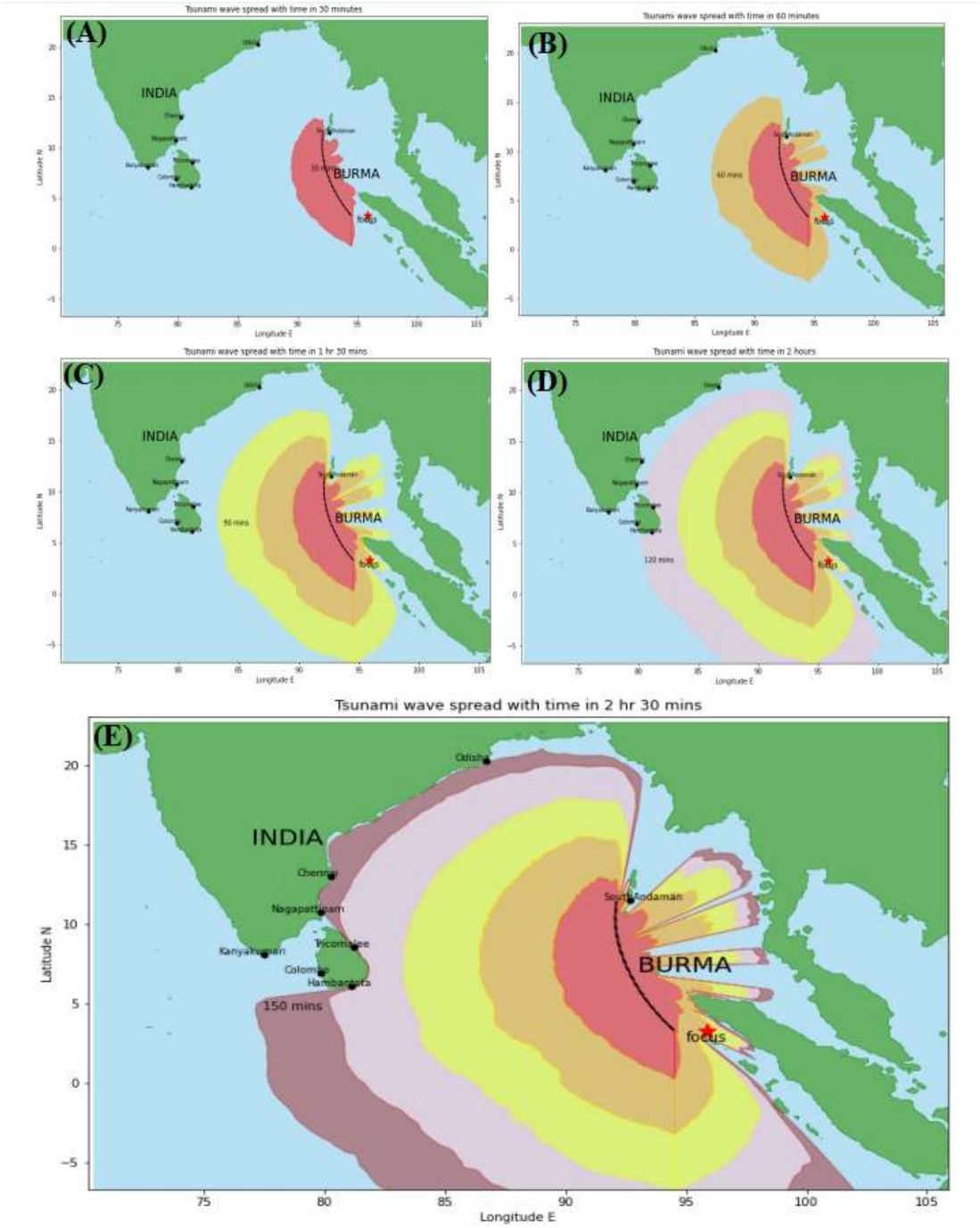

Fig. 10: Simulation results of tsunami wave spread with time for a 2004 Indian Ocean tsunami

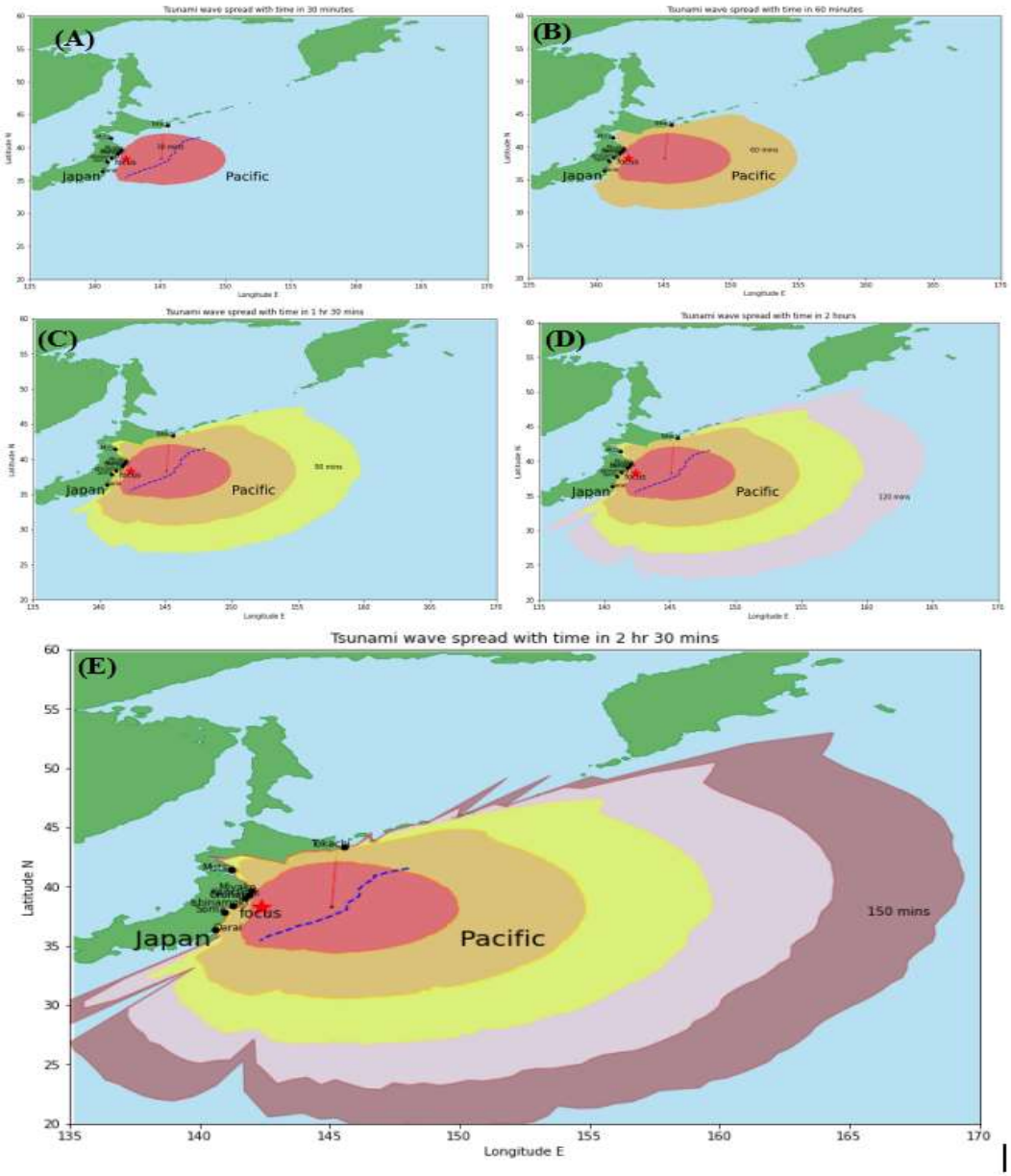

Fig. 17: Simulation results of tsunami wave spread with time for the 2011 Tohoku, Japan tsunami

Table 3. Comparison of historical and modeled tsunami travel times

Sl. No.	Location	Modelled data, hrs	Historical data, hrs	Time difference hh/mm/ss	Accuracy %	References
1	Cocos Island,Australia	2.3386	2.45	0:6:41.4	95	[29]
2	Paradeep	2.47	2.467	0:0:10.8	99	[31]
3	Chennai	2.385	2.583	0:11:52.8	92	[32]
4	Vishakhapatnam	2.512	2.583	0:4:15.6	97	[33]
5	Portblair, Andaman	0.6053	0.667	0:3:42	90	[34]

Table 4. Modeled tsunami wave characteristics data in the specified location for the 2004 Sumatra Andaman earthquake tsunami

Location	**Latitude**	**Longitude**	**Max. wave height (m)**	**Travel time, hh/mm/ss**	**Run-up height (m)**	**Inundation distance(m)**	**References**
Nagapattinam	10.7843	79.8505	12.47	2:22:18	4.38	4400	[33]
Karaikal,Puthucherry	10.9186	79.8532	12.06	2:21:49	5.16	2100	[33]
Kanyakumari	8.078	77.541	11	3:55:10	2.7	500	[33]
Portblair, Andaman	11.675	92.761	7.41	0:36:19	4.17	414	[34]
Chennai	13.0498	80.2823	2.4762	2:23:08	4.3	651	[35]
Cuddalore	11.7399	79.7868	6.17	2:14:37	2.48	404	[35]
Nagore	10.8222	79.84917	4.05	2:21:29	3.059	940	[36]

Table 6. Comparison of tsunami travel time between Modelled data and Historical data

Sl. No.	**Location**	**Modeled data (hours)**	**Observed data (hours)**	**Time difference mm/ss**	**Percentage of accuracy (%)**
1	Tappi	1.32	1.3833	3:48	95
2	Hakodate	1.43	1.4167	0:47	98
3	Muroranko	1.2	1.1667	2:00	97
4	Chichijima Island	1.51	1.4667	2:35	97
5	Yuki	1.79	1.85	3:36	96

Table 7. Modeled tsunami wave characteristics data in the specified location for 2011 Japan, Tohoku tsunami

Location	Latitude (^oN)	Longitude (^oE)	Max. Wave height (m) [51], [52]	Travel Time, hh/mm/ss [51]	Run-up, m [51]	Inundation Distance (m) [51], [52]
Tokachi, Hokkaido	43.35	145.583	18.07	1:16:56	3.614	300
Mutsu, Aomori	41.367	141.233	13.35	1:05:00	7.2	220
Miyako, Iwate	39.65	141.983	10.386	0:37:51	6.3	200
Kamaishi, Iwate	39.267	141.883	10.707	0:32:56	8.1	400
Ofunato, Iwate	39.017	141.75	13.035	0:47:11	6.8	270
Ishinamoki, Miyagi	38.417	141.267	16.01	1:04:16	9	420
Soma, Fukushima	37.833	140.967	16.86	1:08:23	5	560
Oarai, Ibaraki	36.333	140.583	6.92	0:59:03	4.2	380